Sum-Rate Maximization of Uplink Rate Splitting Multiple Access (RSMA) Communication

Zhaohui Yang, *Member, IEEE*, Mingzhe Chen, *Member, IEEE*, Walid Saad, *Fellow, IEEE*, Wei Xu, *Senior Member, IEEE*, and Mohammad Shikh-Bahaei, *Senior Member, IEEE*

Abstract—In this paper, the problem of maximizing the wireless users' sum-rate for uplink rate splitting multiple access (RSMA) communications is studied. In the considered model, the message intended for a single user is split into two sub-messages with separate transmit power and the base station (BS) uses a successive decoding technique to decode the received messages. To maximize each user's transmission rate, the users must adjust their transmit power and the BS must determine the decoding order of the messages transmitted from the users to the BS. This problem is formulated as a sum-rate maximization problem with proportional rate constraints by adjusting the users' transmit power and the BS's decoding order. However, since the decoding order variable in the optimization problem is discrete, the original maximization problem with transmit power and decoding order variables can be transformed into a problem with only the rate splitting variable. Then, the optimal rate splitting of each user is determined. Given the optimal rate splitting of each user and a decoding order, the optimal transmit power of each user is calculated. Next, the optimal decoding order is determined by an exhaustive search method. To further reduce the complexity of the optimization algorithm used for sum-rate maximization in RSMA, a user pairing based algorithm is introduced, which enables two users to use RSMA in each pair and also enables the users in different pairs to be allocated with orthogonal frequency. For comparisons, the optimal sum-rate maximizing solutions with proportional rate constraints are obtained for non-orthogonal multiple access (NOMA), frequency division multiple access (FDMA), and time division multiple access (TDMA). Simulation results show that RSMA can achieve up to 10.0, 22.2, and 81.2 percent gains in terms of sum-rate compared to NOMA, FDMA, and TDMA.

Index Terms—Rate splitting multiple access (RSMA), decoding order, power management, resource allocation

1 Introduction

Driven by the rapid development of advanced multimedia applications in Internet of Things, next-generation wireless networks [2] must support high spectral efficiency and massive connectivity. In consequence, rate splitting multiple access (RSMA)[1] has been recently proposed as an effective approach to provide more general and robust transmission framework compared to non-orthogonal multiple access (NOMA) [3], [4], [5], [6], [7] and space-division multiple access (SDMA). However, implementing RSMA in wireless networks also faces several challenges [8] such as decoding order design and resource management for message transmission.

Recently, a number of existing works such as in [9], [10], [11], [12], [13], [14], [15], [16], [17], [18], [19], [20], [21], [22], [23], [24], [25], [26] have studied several problems related to the implementation of RSMA in wireless networks.The prior works on RSMA focus on two key aspects: downlink transmission and uplink transmission. RSMA for downlink systems includes two special cases: multiuser linear precoding and power-domain NOMA. As such, RSMA can improve downlink rate and quality of service under both perfect channel state information at transmitter (CSIT) [9], [10], [11], [12], [13], [14], [15], [16], [17], [18] and imperfect CSIT [19], [20], [21]. The work in [12] showed that RSMA can achieve better performance than NOMA and SDMA. In [13], the application of linearly-precoded rate splitting is studied for multiple input single output (MISO) simultaneous wireless information and power transfer (SWIPT) broadcast channel systems. The work in [14] developed a transmission scheme that combines rate splitting, common message decoding, clustering and coordinated beamforming so as to maximize the weighted sum-rate of users. In [15] and [16], the energy efficiency of the RSMA networks was studied. The data rate of using RSMA for two-receiver MISO broadcast channel with finite rate feedback was studied in [17]. Our prior work in [18] investigated the power management and rate splitting scheme to maximize the sum-rate of the users. Considering imperfect CSIT, the authors in [19] optimized the system

1. Note that RSMA is also used for resource spread multiple access in 3GPP. In the abbreviation "RSMA", RSMA refers exclusively to abbreviation of rate splitting multiple access.

- *Zhaohui Yang and Mohammad Shikh-Bahaei are with the Centre for Telecommunications Research, Department of Engineering, King's College London, WC2R 2LS London, U.K. E-mail: {yang.zhaohui, m.sbahaei}@kcl.ac.uk.*
- *Mingzhe Chen is with the Electrical Engineering Department, Princeton University, Princeton, NJ 08544 USA, and also with the Chinese University of Hong Kong, Shenzhen, China. E-mail: mzchen00@gmail.com.*
- *Walid Saad is with the Wireless@VT, Bradley Department of Electrical and Computer Engineering, Virginia Tech, Blacksburg, VA 24061 USA. E-mail: walids@vt.edu.*
- *Wei Xu is with the National Mobile Communications Research Lab, Southeast University, Nanjing 210096, China , and also with the Henan Joint International Research Laboratory of Intelligent Networking and Data Analysis, Zhengzhou University, Zhengzhou 450001, China. E-mail: wxu@seu.edu.cn.*

Manuscript received 6 Nov. 2019; revised 23 Sept. 2020; accepted 2 Nov. 2020. Date of publication 12 Nov. 2020; date of current version 3 June 2022.
(Corresponding author: Zhaohui Yang.)
Digital Object Identifier no. 10.1109/TMC.2020.3037374

sum-rate in downlink multi-user multiple input single output (MISO) systems under imperfect CSIT. Moreover, the authors in [20] used RSMA for a downlink multiuser MISO system with bounded errors of CIST. In [21], the authors investigated the rate splitting-based robust transceiver design problem in a multi-antenna interference channel with SWIPT under the norm-bounded errors of CSIT. Motivated by the limitations of conventional multiuser linear precoding assisted non-orthogonal unicast and multicast (NOUM), the authors in [22] studied the application of RSMA in the NOUM transmission. However, most of the existing works such as in [9], [10], [11], [12], [13], [14], [15], [16], [17], [18], [19], [20], [21], [22] studied the use of RSMA for the downlink rather than in the uplink. In fact, using RSMA for uplink data transmission can theoretically achieve the optimal capacity region with perfect CSIT [23]. For uplink RSMA systems, the heuristic scheme was proposed to achieve the same sum rate as that of the belief propagation strategy [24], while the exhaustive searching based scheme was proposed to maximize the minimum data rate [25]. In [26], the outage performance was investigated for uplink RSMA systems. However, none of the existing works in [24], [25], [26] jointly considered the optimization of power management and message decoding order for uplink RSMA. In practical RSMA deployments, the message decoding order will affect the transmission rate of the uplink users and, thus, it must be optimized.

For uplink wireless communications, there are three main methods to achieve the optimum rate region: NOMA with time sharing, joint encoding/decoding, and RSMA [27]. For NOMA with time sharing, the implementation complexity is high since the time sharing transmission requires multiple time slots. Moreover, NOMA with time sharing requires synchronization among users. The joint encoding/decoding based approach is also difficult to implement in practice because random codes have a high decoding complexity. Compared to NOMA with time sharing and joint encoding/decoding methods, RSMA can significantly reduce the implementation complexity [23].

The main difference between uplink RSMA and uplink NOMA is that, in RSMA, there are twice the number of messages for decoding compared to NOMA. In RSMA, the transmitted message of each user is split into two sub-messages. In contrast, in NOMA, the transmitted message of each user is not split. Compared to NOMA, the gain of RSMA comes from the following two aspects. The first aspect is that the number of decoding orders in RSMA is larger than that in NOMA, which shows that RSMA is a robust scheme and NOMA can be viewed as a special case of RSMA. The second aspect is that the rate of each user in RSMA is a sum of two sub-messages, while the rate of each user in NOMA only lies in decoding a single message.

The main contribution of this paper is a novel framework for optimizing power allocation and message decoding for uplink RSMA transmissions. Our key contributions include:

- We consider the uplink of a wireless network that uses RSMA, in which each user transmits a superposition of two messages with different power levels and the base station (BS) uses a SIC technique to decode the received messages. The power allocation and decoding order problem is formulated as an optimization problem whose goal is to maximize the sum-rate of all users under proportional rate constraints.
- The non-convex sum-rate maximization problem with discrete decoding variable and transmit power variable is first transformed into an equivalent problem with only the rate splitting variable. Then, the optimal solution of the rate splitting is obtained. Based on the optimal rate splitting of each user, the optimal transmit power can be derived under a given decoding order. Finally, the optimal decoding order is determined by exhaustive search. For the two-user scenario, the optimal transmit power can be obtained in closed form.To reduce the computational complexity, a low-complexity RSMA scheme based on user pairing is proposed to show near sum-rate performance of RSMA without user pairing.
- We provide optimal solutions for sum-rate maximization problems in uplink NOMA, frequency division multiple access (FDMA), and time division multiple access (TDMA). Simulation results show that RSMA achieves better performance than NOMA, FDMA, and TDMA in terms of sum-rate.

The rest of this paper is organized as follows. The system model and problem formulation are described in Section 2. The optimal solution is presented in Section 3. Section 4 presents a low-complexity sum-rate maximization scheme. The optimal solutions of sum-rate maximization for NOMA, FDMA and TDMA are provided in Section 5. Simulation results are analyzed in Section 6. Conclusions are drawn in Section 7.

2 System Model and Problem Formulation

Consider a single cell uplink network with one BS serving a set $\mathcal{K}$ of K users using RSMA. In a practical RSMA system, the message intended for a single user is split into two sub-messages. Then, rate splitting is achieved by allocating two different powers to these two sub-messages, as shown in Fig. 1. Then, the BS uses a SIC technique to decode the messages of all users [23]. Since the message of each user is split into two sub-messages, the rate of each user is also split into two sub-rates.

The transmitted message s_k of user $k \in \mathcal{K}$ is split into two sub-messages s_{k1} and s_{k2}, which is given by:

$$s_k = \sum_{j=1}^{2} \sqrt{p_{kj}} s_{kj}, \quad \forall k \in \mathcal{K}, \tag{1}$$

where p_{kj} is the transmit power of sub-message s_{kj} from user k.

The total received message s_0 at the BS can be given by:

$$s_0 = \sum_{k=1}^{K} \sqrt{h_k} s_k + n = \sum_{k=1}^{K} \sum_{j=1}^{2} \sqrt{h_k p_{kj}} s_{kj} + n, \tag{2}$$

where h_k is the channel gain between user k and the BS and n is the additive white Gaussian noise. Each user k has a maximum transmission power limit P_k, i.e., $\sum_{j=1}^{2} p_{kj} \leq P_k$.

To decode all messages s_{kj} from the received message s_0, the BS will use SIC. The decoding order at the BS is denoted by a permutation $\boldsymbol{\pi}$. The permutation $\boldsymbol{\pi}$ belongs to set Π

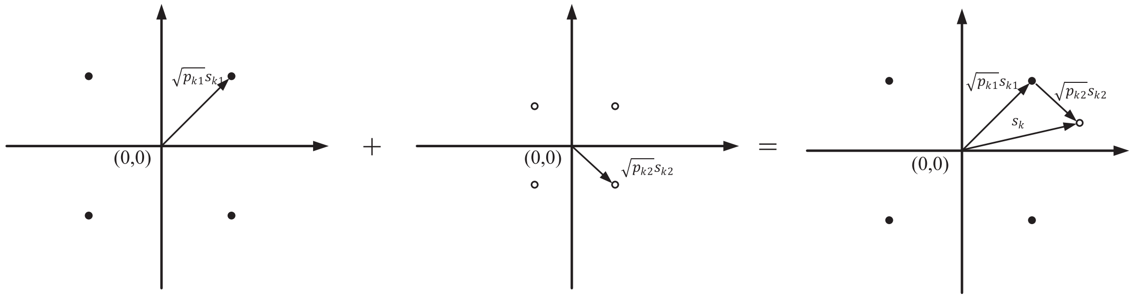

(a) Signal constellation of sub-message s_{k1} (b) Signal constellation of sub-message s_{k2} (c) Signal constellation of transmitted signal s_k

Fig. 1. An example of rate splitting.

defined as the set of all possible decoding orders of all $2K$ messages from K users. The decoding order of message s_{kj} from user k is π_{kj}. The achievable rate of decoding message s_{kj} is:

$$r_{kj} = B\log_2\left(1+\frac{h_k p_{kj}}{\sum_{\{(l\in\mathcal{K},m\in\mathcal{J})|\pi_{lm}>\pi_{kj}\}} h_l p_{lm}+\sigma^2 B}\right), \tag{3}$$

where B is the bandwidth of the BS, σ^2 is the power spectral density of the Gaussian noise. The set $\{(l\in\mathcal{K}, m\in\mathcal{J})|\pi_{lm} > \pi_{kj}\}$ in (3) represents the sub-messages s_{lm} that are decoded after message s_{kj}.

Since the transmitted message of user k includes messages s_{k1} and s_{k2}, the achievable rate of user k is given by:

$$r_k = \sum_{j=1}^{2} r_{kj}. \tag{4}$$

Our objective is to maximize the sum-rate of all users with proportional rate constraints. Mathematically, the sum-rate maximization problem can be formally posed as follows:

$$\max_{\boldsymbol{\pi},\boldsymbol{p}} \quad \sum_{k=1}^{K} r_k, \tag{5}$$

$$\text{s.t.} \quad r_1 : r_2 : \cdots : r_K = D_1 : D_2 : \cdots D_K, \tag{5a}$$

$$\sum_{j=1}^{2} p_{kj} \le P_k, \quad \forall k\in\mathcal{K}, \tag{5b}$$

$$\boldsymbol{\pi}\in\Pi, p_{kj}\ge 0, \quad \forall k\in\mathcal{K}, j\in\mathcal{J}, \tag{5c}$$

$$\sum_{k=1}^{K}\sum_{j=1}^{2} p_{kj} \le P_{\max}, \tag{5d}$$

where $\boldsymbol{p} = [p_{11}, p_{12}, \ldots, p_{K1}, p_{K2}]^T$, r_k is defined in (4), $\mathcal{J} = \{1,2\}$, and $P_{\max}$ is the maximum total power of all users. $D_1, \ldots, D_K$ is a set of predetermined nonnegative values that are used to ensure proportional fairness among users. The value of D_k represents the proportional fairness among users, i.e., large D_k means that user k would achieve high data rate. In practical, the value of D_k is selected based on the data rate requirement, and large D_k is selected for the user with high data rate requirement. For the special case with equal D_k, i.e., $D_1 = D_2 = \cdots = D_K$, all users would achieve the same data rate. The fairness index is defined as

$$\frac{\left(\sum_{k=1}^{K} D_k\right)^2}{K\sum_{k=1}^{K} D_k^2}, \tag{6}$$

with the maximum value of 1 to be the greatest fairness case in which all users would achieve the same data rate [28]. The fairness index given in (6) is called the Jain's fairness index [29].With proper unitization, we set

$$\sum_{k=1}^{K} D_k = 1. \tag{7}$$

In RSMA, the rate is sensitive to power allocation and tight power control is necessary. Here, we consider a block fading channel. For each block fading time (for example 1 s [30]), the channel gains between all users and the BS do not change. Note that the data size of each power value is small (usually less than 20 bits) and the transmission power of the BS is higher than the users. Since only two power values need to be signalled to each user over a downlink channel, the transmission time for power value transmission is small compared to the block time. As a result, the rate degradation of considering the power value transmission is marginal.

Although it was stated in [23] that RSMA can reach the optimal rate region, no practical algorithm was proposed to compute the decoding order and power allocation. It is therefore necessary to quantify the uplink performance gains that RSMA can obtain compared to conventional multiple access schemes.

Due to the non-linear equality constraint (5a) and discrete variable $\boldsymbol{\pi}$, problem (5) is a non-convex mixed integer problem. Hence, it is generally hard to solve problem (5). Despite the non-convexity and discrete variable, we will next develop a novel algorithm to obtain the globally optimal solution to problem (5).

3 Optimal Power Allocation and Decoding Order

In this section, an effective algorithm is proposed to obtain the optimal power allocation and decoding order of sum-rate maximization problem (5). To solve problem (5), we first obtain the optimal fair rate by solving an equivalent problem. With the optimal fair rate, problem (5) reduces to a feasibility problem of decoding order and power allocation. The decoding order is solved by the exhaustive search method and the power allocation is obtained by using the difference of two convex function (DC) method. The proposed process for solving problem (8) in Section 3 is summarized in Fig. 2.

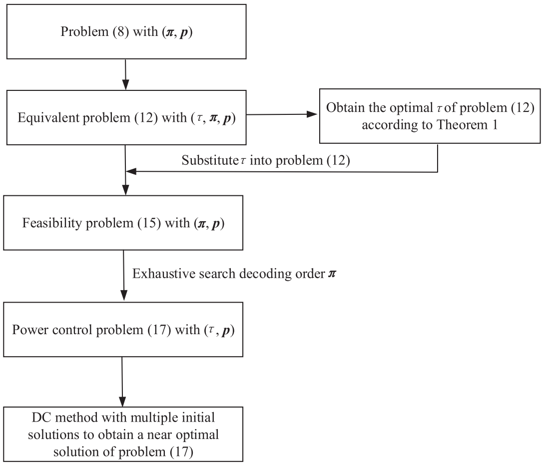

Fig. 2. Proposed approach for solving problem (8).

3.1 Optimal Sum-Rate Maximization

Let τ be the sum-rate of all K users. Given this new variable τ, problem (5) can be rewritten as:

$$\max_{\tau,\boldsymbol{\pi},\boldsymbol{p}} \quad \tau, \tag{8}$$

$$\text{s.t.} \quad r_k = D_k\tau, \quad \forall k \in \mathcal{K}, \tag{8a}$$

$$\sum_{j=1}^{2} p_{kj} \le P_k, \quad \forall k \in \mathcal{K}, \tag{8b}$$

$$\boldsymbol{\pi} \in \Pi, p_{kj} \ge 0, \quad \forall k \in \mathcal{K}, j \in \mathcal{J}, \tag{8c}$$

$$\sum_{k=1}^{K}\sum_{j=1}^{2} p_{kj} \le P_{\max}, \tag{8d}$$

where τ is the sum-rate of all users since $\tau = \sum_{k=1}^{K} D_k\tau = \sum_{k=1}^{K} r_k$ according to (7) and (8a).

Problem (8) is challenging to solve due to the decoding order variable $\boldsymbol{\pi}$ with discrete value space. To handle this difficulty, we provide the following lemma, which can be used for transforming problem (8) into an equivalent problem without decoding order variable $\boldsymbol{\pi}$.

Lemma 1. *In RSMA, under a proper decoding order $\boldsymbol{\pi}$ and splitting power allocation $\boldsymbol{p}$, the optimal rate region can be fully achieved, i.e.,*

$$\sum_{k\in\mathcal{K}'} r_k \le B\log_2\left(1+\frac{\sum_{k\in\mathcal{K}'} h_k q_k}{\sigma^2 B}\right), \quad \forall \mathcal{K}' \subseteq \mathcal{K}\setminus\emptyset, \tag{9}$$

where

$$0 \le q_k \le P_k, \sum_{k=1}^{K} q_k \le P_{\max}, \quad \forall k \in \mathcal{K}, \tag{10}$$

q_k stands for the sum transmit power of user k, and $\emptyset$ is an empty set and $\mathcal{K}' \subseteq \mathcal{K}\setminus\emptyset$ means that $\mathcal{K}'$ is a non-empty subset of $\mathcal{K}$.

Lemma 1 follows directly from [23, Theorem 1]. Based on Lemma 1, we can use the rate variable to replace the power and decoding variables. In consequence, problem (8) can be equivalently transformed to

$$\max_{\tau,\boldsymbol{r},\boldsymbol{q}} \quad \tau, \tag{11}$$

$$\text{s.t.} \quad r_k = D_k\tau, \quad \forall k \in \mathcal{K}, \tag{11a}$$

$$\sum_{k\in\mathcal{K}'} r_k \le B\log_2\left(1+\frac{\sum_{k\in\mathcal{K}'} h_k q_k}{\sigma^2 B}\right), \forall \mathcal{K}' \subseteq \mathcal{K}\setminus\emptyset, \tag{11b}$$

$$0 \le q_k \le P_k, \sum_{k=1}^{K} q_k \le P_{\max}, \quad \forall k \in \mathcal{K}, \tag{11c}$$

where $\boldsymbol{r} = [r_1, r_2, \ldots, r_K]^T$ and $\boldsymbol{q} = [q_1, q_2, \ldots, q_K]^T$. In problem (11), the dimension of the variable is smaller than that in problem (8). Moreover, the discrete decoding order variable is replaced by rate variable in problem (11). Regarding the optimal solution of problem (11), we have the following lemma.

Lemma 2 *For the optimal solution $(\tau^*, \boldsymbol{r}^*, \boldsymbol{q}^*)$ of problem (11), there exists at least one $\mathcal{K}' \subseteq \mathcal{K}\setminus\emptyset$ such that $\sum_{k\in\mathcal{K}'} r_k^* = B\log_2(1+\frac{\sum_{k\in\mathcal{K}'} h_k q_k^*}{\sigma^2 B})$.*

Proof. See Appendix A, which can be found on the Computer Society Digital Library at http://doi.ieeecomputersociety.org/10.1109/TMC.2020.3037374. □

Lemma 2 indicates the optimal condition for the optimal solution. Based on this optimal condition, the optimal solution of problem (11) can be obtained using the following theorem.

Theorem 1 *The optimal solution of problem (11) is*

$$\tau^* = \min_{\mathcal{K}'\subseteq\mathcal{K}\setminus\emptyset} \frac{B\log_2\left(1+\frac{\sum_{k\in\mathcal{K}'} h_k q_k^*}{\sigma^2 B}\right)}{\sum_{k\in\mathcal{K}'} D_k}, \tag{12}$$

and

$$r_k^* = D_k \min_{\mathcal{K}'\subseteq\mathcal{K}\setminus\emptyset} \frac{B\log_2\left(1+\frac{\sum_{k\in\mathcal{K}'} h_k q_k^*}{\sigma^2 B}\right)}{\sum_{k\in\mathcal{K}'} D_k}, \quad \forall k \in \mathcal{K}, \tag{13}$$

where $\boldsymbol{q}^*$ is the optimal solution to the following convex problem:

$$\max_{\boldsymbol{q}} \quad \min_{\mathcal{K}'\subseteq\mathcal{K}\setminus\emptyset} \frac{B\log_2\left(1+\frac{\sum_{k\in\mathcal{K}'} h_k q_k}{\sigma^2 B}\right)}{\sum_{k\in\mathcal{K}'} D_k} \tag{14a}$$

$$\text{s.t.} \quad 0 \le q_k \le P_k, \sum_{k=1}^{K} q_k \le P_{\max}, \quad \forall k \in \mathcal{K}. \tag{14b}$$

Proof. See Appendix B, available in the online supplemental material. □

From (12), one can directly obtain the optimal sum-rate of problem (11) in closed form, which can be helpful in characterizing the rate performance of RSMA.

Having obtained the optimal solution $(\tau^*, \boldsymbol{r}^*, \boldsymbol{q}^*)$ of problem (11), we still need to calculate the optimal $(\boldsymbol{\pi}^*, \boldsymbol{p}^*)$ of the original problem (8). Next, we introduce a new algorithm to obtain the optimal $(\boldsymbol{\pi}^*, \boldsymbol{p}^*)$ of problem (8).

Substituting the optimal solution $(\tau^*, \boldsymbol{r}^*, \boldsymbol{q}^*)$ of problem (11) into problem (8), we can obtain the following feasibility problem:

$$\text{find} \quad \boldsymbol{\pi}, \boldsymbol{p}, \tag{15}$$

$$\text{s.t.} \quad \sum_{j=1}^{2} B \log_2\left(1 + \frac{h_k p_{kj}}{\sum_{\{(l\in\mathcal{K}, m\in\mathcal{J})|\pi_{lm}>\pi_{kj}\}} h_l p_{lm} + \sigma^2 B}\right) = r_k^*, \quad \forall k \in \mathcal{K}, \tag{15a}$$

$$\sum_{j=1}^{2} p_{kj} = q_k^*, \quad \forall k \in \mathcal{K}, \tag{15b}$$

$$\boldsymbol{\pi} \in \Pi, p_{kj} \geq 0, \quad \forall k \in \mathcal{K}, j \in \mathcal{J}. \tag{15c}$$

Due to the decoding order constraint (15c), it is challenging to find the optimal solution of problem (15). To solve this problem, we first fix the decoding order $\boldsymbol{\pi}$ to obtain the power allocation and then exhaustively search $\boldsymbol{\pi}$. Given decoding order $\boldsymbol{\pi}$, problem (15) can be simplified as:

$$\text{find} \quad \boldsymbol{p}, \tag{16}$$

$$\text{s.t.} \quad \sum_{j=1}^{2} B \log_2\left(1 + \frac{h_k p_{kj}}{\sum_{\{(l\in\mathcal{K}, m\in\mathcal{J})|\pi_{lm}>\pi_{kj}\}} h_l p_{lm} + \sigma^2 B}\right) \geq r_k^*, \quad \forall k \in \mathcal{K}, \tag{16a}$$

$$\sum_{j=1}^{2} p_{kj} = q_k^*, \quad \forall k \in 1\mathcal{K}, \tag{16b}$$

$$p_{kj} \geq 0, \quad \forall k \in \mathcal{K}, j \in \mathcal{J}. \tag{16c}$$

Note that the equality in (15a) is replaced by the inequality in (16a). The reason is that any feasible solution to problem (15) is also feasible to problem (16). Meanwhile, for a feasible solution to problem (16), we can always construct a feasible solution to problem (15).

To verify the feasibility of problem (16), we can construct the following problem by introducing a new variable α:

$$\max_{\alpha, \boldsymbol{p}} \quad \alpha, \tag{17}$$

$$\text{s.t.} \quad \sum_{j=1}^{2} B \log_2\left(1 + \frac{h_k p_{kj}}{\sum_{\{(l\in\mathcal{K}, m\in\mathcal{J})|\pi_{lm}>\pi_{kj}\}} h_l p_{lm} + \sigma^2 B}\right) \geq \alpha r_k^*, \quad \forall k \in \mathcal{K}, \tag{17a}$$

$$\sum_{j=1}^{2} p_{kj} = q_k^*, \quad \forall k \in \mathcal{K}, \tag{17b}$$

$$p_{kj}, \alpha \geq 0, \quad \forall k \in \mathcal{K}, j \in \mathcal{J}. \tag{17c}$$

To show the equivalence between problems (16) and (17), we provide the following lemma.

Lemma 3. *Problem (16) is feasible if and only if the optimal objective value α^* of problem (17) is equal to or larger than 1.*

Proof. See Appendix C, available in the online supplemental material. □

Based on Lemma 3, the feasibility problem (16) is equivalent to problem (17). Problem (17) is non-convex due to constraints (17a). To handle the non-convexity of (17), we adopt the DC method, using which a non-convex problem can be solved suboptimally by converting a non-convex problem into convex subproblems. In order to obtain a near globally optimal solution of problem (17), we can try multiple initial points $(\alpha, \boldsymbol{p})$, which can lead to multiple locally optimal solutions. Thus, a near globally optimal solution can be obtained by choosing the locally optimal solution with the highest objective value among all locally optimal solutions. To construct an initial feasible point, we first arbitrarily generate $\boldsymbol{p}$ that satisfies linear constraints (17b) and (17c), and then we set:

$$\alpha = \min_{k\in\mathcal{K}} \frac{\sum_{j=1}^{2} B \log_2\left(1 + \frac{h_k p_{kj}}{\sum_{\{(l\in\mathcal{K}, m\in\mathcal{J})|\pi_{lm}>\pi_{kj}\}} h_l p_{lm} + \sigma^2 B}\right)}{r_k^*}. \tag{18}$$

By using the DC method, the left hand side of (17a) satisfies:

$$\sum_{j=1}^{2} B \log_2\left(1 + \frac{h_k p_{kj}}{\sum_{\{(l\in\mathcal{K}, m\in\mathcal{J})|\pi_{lm}>\pi_{kj}\}} h_l p_{lm} + \sigma^2 B}\right) \tag{19}$$

$$= \sum_{j=1}^{2} B \log_2\left(\sum_{\{(l\in\mathcal{K}, m\in\mathcal{J})|\pi_{lm}\geq\pi_{kj}\}} h_l p_{lm} + \sigma^2 B\right) - \sum_{j=1}^{2} B \log_2\left(\sum_{\{(l\in\mathcal{K}, m\in\mathcal{J})|\pi_{lm}>\pi_{kj}\}} h_l p_{lm} + \sigma^2 B\right) \tag{20}$$

$$\geq \sum_{j=1}^{2} B \log_2\left(\sum_{\{(l\in\mathcal{K}, m\in\mathcal{J})|\pi_{lm}\geq\pi_{kj}\}} h_l p_{lm} + \sigma^2 B\right) - \sum_{j=1}^{2} B \log_2\left(\sum_{\{(l\in\mathcal{K}, m\in\mathcal{J})|\pi_{lm}>\pi_{kj}\}} h_l p_{lm}^{(n)} + \sigma^2 B\right) - \sum_{j=1}^{2} B \frac{\sum_{\{(l\in\mathcal{K}, m\in\mathcal{J})|\pi_{lm}>\pi_{kj}\}} h_l (p_{lm} - p_{lm}^{(n)})}{(\ln 2) \sum_{\{(l\in\mathcal{K}, m\in\mathcal{J})|\pi_{lm}>\pi_{kj}\}} h_l p_{lm}^{(n)} + \sigma^2 B} \tag{21}$$

$$\triangleq r_{k,\text{lb}}(\boldsymbol{p}, \boldsymbol{p}^{(n)}), \tag{22}$$

where $p_{lm}^{(n)}$ represents the value of p_{lm} at iteration n, and the inequality follows from the fact that $\log_2(x)$ is a concave function and a concave function is always no greater than its first-order approximation. Note that the value of (20) is not always zero since

$$\sum_{\{(l\in\mathcal{K}, m\in\mathcal{J})|\pi_{lm}\geq\pi_{kj}\}} h_l p_{lm} + \sigma^2 B \geq \sum_{\{(l\in\mathcal{K}, m\in\mathcal{J})|\pi_{lm}>\pi_{kj}\}} h_l p_{lm} + \sigma^2 B. \tag{23}$$

By substituting the left term of constraints (17a) with the concave function $r_{k,\text{lb}}(\boldsymbol{p}, \boldsymbol{p}^{(n)})$, problem (17) becomes convex, and can be effectively solved by the interior point method [31].

The near optimal sum-rate maximization algorithm for RSMA is provided in Algorithm 1, where N is the number of initial points to obtain a near globally optimal solution of non-convex problem (17). In Algorithm 1, the optimal fair rate is obtained by using Theorem 1 at step 1. At step 2, the decoding order is exhaustively searched and the technique for decoding order is given in Section 3.2. At step 3, the DC method is operated N times and i means the ith time of running DC method. The initial solution of problem (17) is randomly generated during step 4. The DC procedures are given in steps 5-7. The near globally optimal solution is obtained by choosing the highest objective value among N locally optimal solutions at step 9. At step 10, α^* is updated when the decoding order is changed. The optimal solution is found if $\alpha^* = 1$ as shown in step 11. At step 13, the solutions are obtained.

Algorithm 1. Near Optimal Sum-Rate Maximization for RSMA

1: Obtain the optimal solution $(\boldsymbol{\tau}^*, \boldsymbol{r}^*, \boldsymbol{q}^*)$ of problem (11) according to Theorem 1. Initialize $\alpha^* = 0$.
2: **for** $\boldsymbol{\pi} \in \Pi$ **do**
3:   **for** $i : 1 : N$ **do**
4:     Arbitrarily generate a feasible solution $(\boldsymbol{\alpha}^{(0)}, \boldsymbol{p}^{(0)})$ of problem (17), and set $n = 0$.
5:     **repeat**
6:       Obtain the optimal solution $(\boldsymbol{\alpha}^{(n+1)}, \boldsymbol{p}^{(n+1)})$ of convex problem (17) by replacing the left term of constraints (17a) with $r_{k,\mathrm{lb}}(\boldsymbol{p}, \boldsymbol{p}^{(n)})$. Set $n = n + 1$.
7:     **until** the objective value (17a) converges.
8:   **end for**
9:   Obtain the near globally optimal solution $(\bar{\alpha}, \bar{\boldsymbol{p}})$ of problem (17) with the highest objective value.
10:   $\alpha^* = \max\{\alpha^*, \bar{\alpha}\}$.
11:   If $\alpha^* = 1$, break and jump to step 13.
12: **end for**
13: Output decoding order $\boldsymbol{\pi}^* = \boldsymbol{\pi}$ and power allocation $\boldsymbol{p}^* = \bar{\boldsymbol{p}}$ of problem (15).

3.2 Complexity Analysis

In Algorithm 1, the major complexity lies in solving problem (11) and problem (15). To solve (11), from Theorem 1, the complexity is $\mathcal{O}(2^K - 1)$ since the set $\mathcal{K}$ has $2^K - 1$ nonempty subsets. According to steps 2-12, a near globally optimal solution of problem (15) is obtained via solving a series of convex problems with different initial points and decoding order strategies. Considering that the dimension of variables in problem (17) is $1 + 2K$, the complexity of solving convex problem in step 6 by using the standard interior point method is $\mathcal{O}(K^3)$ [31, Pages 487, 569]. Since the network consists of K users and each user transmits a superposition two messages (there are $2K$ messages in total), the decoding order set Π consists of $(2K)!/2^K$ elements. Given N initial points, the total complexity of solving problem (15) is $\mathcal{O}(NK^3(2K)!/2^K)$. As a result, the total complexity of Algorithm 1 is $\mathcal{O}(2^K + NK^3(2K)!/2^K)$.

Due to high complexity of exhaustive search for the decoding order in Algorithm 1, we consider a specific decoding order: $s_{K1}, s_{(K-1)1}, \ldots, s_{11}, s_{12}, \ldots, s_{(K-1)2}, s_{K2}$. Under this given decoding order, the complexity of Algorithm 1 is reduced to $\mathcal{O}(2^K + NK^3)$. The intuition of choosing this decoding order is as follow. The optimal decoding order for a two-user case is s_{21}, s_{11}, s_{22} according to Section 3.3, and we use this structure to construct decoding order $s_{K1}, s_{(K-1)1}, \ldots, s_{11}, s_{12}, \ldots, s_{(K-1)2}, s_{K2}$ for the general multi-user case. Note that this decoding order is not always the optimal decoding order.

In practice, we consider small K to reduce the SIC complexity, the computational complexity of Algorithm 1 can be practical. To deal with a large number of users, the users can be classified into different groups with small number of users in each group. The users in different groups occupy different frequency bands and users in the same group are allocated to the same frequency band using RSMA [32], [33].

3.3 RSMA With Two Users

Based on Lemma 1, the rate region of RSMA with two users can be expressed by:

$$\{(r_1, r_2) | 0 \le r_1 \le R_1, 0 \le r_2 \le R_2, r_1 + r_2 \le R_{\max}\}, \tag{24}$$

where

$$R_1 = B \log_2\left(1 + \frac{h_1 q_1}{\sigma^2 B}\right), \tag{25}$$

$$R_2 = B \log_2\left(1 + \frac{h_2 q_2}{\sigma^2 B}\right), \tag{26}$$

$$R_{\max} = B \log_2\left(1 + \frac{h_1 q_1 + h_2 q_2}{\sigma^2 B}\right). \tag{27}$$

According to Algorithm 1, the computational complexity needed to obtain the boundary point (as shown in Lemma 2 the optimal point to minimize always lies in the boundary point) of the rate region for RSMA is high. In the following, we introduce a low-complexity method to obtain all boundary points of the rate region in two-user RSMA.

In two-user RSMA, only one user needs to transmit a superposition code of two messages and the other user transmits one message. Without loss of generality, user 1 only transmits one message s_{11}, i.e., the transmit power for message s_{12} is always 0.

Lemma 4. *For two-user RSMA, the optimal decoding order is s_{21}, s_{11} and s_{22}. For the boundary rate (r_1, r_2), we consider the following three cases.*

Case (1) $r_1 = R_1$, $0 \le r_2 \le R_{\max} - R_1$: the optimal power allocation is

$$p_{11} = q_1, p_{12} = 0, \tag{28}$$

$$p_{21} = \frac{1}{h_2}\left(2^{\frac{r_2}{B}} - 1\right)(h_1 q_1 + \sigma^2 B), p_{22} = 0. \tag{29}$$

Case (2) $r_2 = R_2$, $0 \le r_1 \le R_{\max} - R_2$: the optimal power allocation is

$$p_{11} = \frac{1}{h_1}\left(2^{\frac{r_1}{B}} - 1\right)(h_2 q_2 + \sigma^2 B), p_{12} = 0, \tag{30}$$

$$p_{21} = 0, p_{22} = q_2. \tag{31}$$

Case (3) $r_1 + r_2 = R_{\max}$, $0 \le r_1 \le R_1$, $0 \le r_2 \le R_2$: the optimal power allocation is

$$p_{11}=q_1, p_{12}=0, p_{21}=q_2-\frac{h_1q_1}{h_2\left(2^{\frac{r_1}{B}}-1\right)}+\frac{\sigma^2 B}{h_2}, \tag{32}$$

$$p_{22}=\frac{h_1q_1}{h_2\left(2^{\frac{r_1}{B}}-1\right)}-\frac{\sigma^2 B}{h_2}. \tag{33}$$

Proof: See Appendix D, available in the online supplemental material. □

According to Lemma 4, the optimal decoding order and power control can be obtained in closed form for the simple two-user case.

4 Low-Complexity Sum-Rate Maximization

According to Section 3.2, the computational complexity of sum-rate maximization for RSMA is extremely high. In this section, we propose a low-complexity scheme for RSMA, where users are classified into different pairs[2] and each pair consists of two users. RSMA is used in each pair and different pairs are allocated with different frequency bands. Assume that K users are classified into M pairs, i.e., $K=2M$. The set of all pairs is denoted by $\mathcal{M}$.

For pair m, the allocated fraction of bandwidth is denoted by f_m. Let c_{mj} denote the data rate of user j in pair m. According to Lemma 1, we have:

$$c_{mj}\leq Bf_m\log_2\left(1+\frac{h_{mj}q_{mj}}{\sigma^2 Bf_m}\right), \quad j\in\mathcal{J}, \tag{34}$$

$$c_{m1}+c_{m2}\leq Bf_m\log_2\left(1+\frac{h_{m1}q_{m1}+h_{m2}q_{m2}}{\sigma^2 Bf_m}\right), \tag{35}$$

where h_{mj} denotes the channel gain between user j in pair m and the BS, and q_{mj} is the transmission power of user j in pair m.

Similar to (5), the sum-rate maximization problem for RSMA with user pairing can be formulated as:

$$\max_{\boldsymbol{f},\boldsymbol{c},\bar{\boldsymbol{q}}} \quad \sum_{m=1}^{M}\sum_{j=1}^{2}c_{mj}, \tag{36}$$

$$\text{s.t.}\quad c_{11}:c_{12}:\cdots:c_{M2}=D_{11}:D_{12}:\cdots:D_{M2} \tag{36a}$$

$$\sum_{m=1}^{M}f_m=1, \tag{36b}$$

$$c_{mj}\leq Bf_m\log_2\left(1+\frac{h_{mj}q_{mj}}{\sigma^2 Bf_m}\right), \forall m\in\mathcal{M}, j\in\mathcal{J}, \tag{36c}$$

$$c_{m1}+c_{m2}\leq Bf_m\log_2\left(1+\frac{h_{m1}q_{m1}+h_{m2}q_{m2}}{\sigma^2 Bf_m}\right), \forall m\in\mathcal{M}, \tag{36d}$$

$$f_m, c_{m1}, c_{m2}\geq 0, \quad \forall m\in\mathcal{M}, \tag{36e}$$

$$0\leq q_{mj}\leq P_{mj}, \sum_{m=1}^{M}\sum_{j=1}^{2}q_{mj}\leq P_{\max}, \quad \forall m, j, \tag{36f}$$

where $\boldsymbol{f}=[f_1,f_2,\ldots,f_M]^T$, $\boldsymbol{c}=[c_{11},c_{12},\ldots,c_{M1},c_{M2}]^T$, $\bar{\boldsymbol{q}}=[q_{11},q_{12},\ldots,q_{M1},q_{M2}]^T$, P_{mj} is the maximum transmit power of user j in pair m, and $D_{11},D_{12},\ldots,D_{M1},D_{M2}$ is a set of predetermined nonnegative values that are used to ensure proportional fairness among users with $\sum_{m=1}^{M}\sum_{j=1}^{2}D_{mj}=1$.

Introducing a new variable τ, problem (36) can be rewritten as:

$$\max_{\tau,\boldsymbol{f},\boldsymbol{c},\bar{\boldsymbol{q}}} \quad \tau, \tag{37}$$

$$\text{s.t.}\quad c_{mj}=D_{mj}\tau, \quad \forall m\in\mathcal{M}, j\in\mathcal{J}, \tag{37a}$$

$$\sum_{m=1}^{M}f_m=1, \tag{37b}$$

$$c_{mj}\leq Bf_m\log_2\left(1+\frac{h_{mj}q_{mj}}{\sigma^2 Bf_m}\right), \forall m\in\mathcal{M}, j\in\mathcal{J}, \tag{37c}$$

$$c_{m1}+c_{m2}\leq Bf_m\log_2\left(1+\frac{h_{m1}q_{m1}+h_{m2}q_{m2}}{\sigma^2 Bf_m}\right), \forall m\in\mathcal{M}, \tag{37d}$$

$$f_m, c_{m1}, c_{m2}\geq 0, \quad \forall m\in\mathcal{M}, \tag{37e}$$

$$0\leq q_{mj}\leq P_{mj}, \sum_{m=1}^{M}\sum_{j=1}^{2}q_{mj}\leq P_{\max}, \quad \forall m, j. \tag{37f}$$

To solve problem (37), we can use the bisection method to obtain the optimal solution. Denote the optimal objective value of problem (37) by τ^*.

We can conclude that problem (37) is always feasible with $\tau<\tau^*$ and infeasible with $\tau>\tau^*$. This motivates us to use the bisection method to find the optimal τ^*, as shown in Fig. 3, where $\tau^{(n)}$ is the value of τ in the nth iteration and $[\tau_{\min},\tau_{\max}]$ is the initial value interval of τ. To show the feasibility of problem (37) for each given τ, we solve a feasibility problem with constraints (37a), (37b), (37c), (37d), and (37 e). With given τ, the feasibility problem of (37) becomes

$$\text{find} \quad \boldsymbol{f},\boldsymbol{c},\bar{\boldsymbol{q}}, \tag{38}$$

$$\text{s.t.}\quad c_{mj}=D_{mj}\tau, \quad \forall m\in\mathcal{M}, j\in\mathcal{J}, \tag{38a}$$

$$\sum_{m=1}^{M}f_m=1, \tag{38b}$$

$$c_{mj}\leq Bf_m\log_2\left(1+\frac{h_{mj}q_{mj}}{\sigma^2 Bf_m}\right), \forall m\in\mathcal{M}, j\in\mathcal{J}, \tag{38c}$$

$$c_{m1}+c_{m2}\leq Bf_m\log_2\left(1+\frac{h_{m1}q_{m1}+h_{m2}q_{m2}}{\sigma^2 Bf_m}\right), \forall m\in\mathcal{M}, \tag{38d}$$

$$f_m, c_{m1}, c_{m2}\geq 0, \quad \forall m\in\mathcal{M}, \tag{38e}$$

$$0\leq q_{mj}\leq P_{mj}, \sum_{m=1}^{M}\sum_{j=1}^{2}q_{mj}\leq P_{\max}, \quad \forall m, j. \tag{38f}$$

Substituting (38a) into (38c) and (38d), we have:

$$D_{mj}\tau\leq Bf_m\log_2\left(1+\frac{h_{mj}q_{mj}}{\sigma^2 Bf_m}\right), \quad j\in\mathcal{J}, \tag{39}$$

2. In this paper, we assume that the user pairing is given, which can be obtained according to matching theory [32] or the order of channel gains [33].

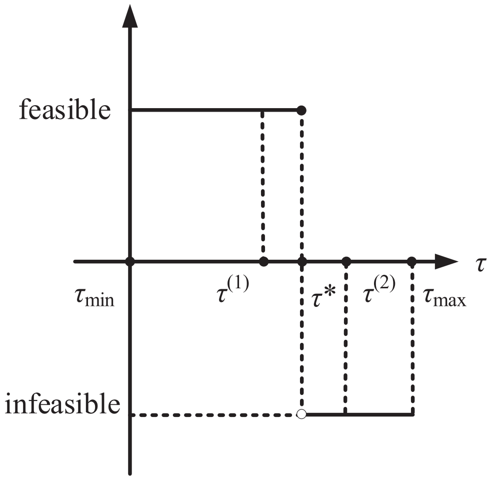

Fig. 3. An illustration of the bisection method.

$$(D_{m1}+D_{m2})\tau \leq Bf_m \log_2\left(1+\frac{h_{m1}q_{m1}+h_{m2}q_{m2}}{\sigma^2 B f_m}\right). \tag{40}$$

It can be proved that $g(x)=x\ln\left(1+\frac{1}{x}\right)$ is a monotonically increasing and also concave function. Thus, to satisfy (39) and (40), bandwidth fraction f_m should satisfy:

$$f_m \geq \max\{f_{m1}(\bar{\boldsymbol{q}}), f_{m2}(\bar{\boldsymbol{q}}), f_{m3}(\bar{\boldsymbol{q}})\}, \tag{41}$$

where

$$f_{mk}(\bar{\boldsymbol{q}}) = -\frac{(\ln 2)D_{mk}h_{mk}q_{mk}}{\kappa_1+(\ln 2)D_{mk}\sigma^2 B}, \quad k=1,2, \tag{42}$$

$$\kappa_1 = Bh_{mk}P_{mk}\tau W\left(-\frac{(\ln 2)D_{mk}\sigma^2}{h_{mk}q_{mk}\tau}\mathrm{e}^{-\frac{(\ln 2)D_{mk}\sigma^2}{h_{mk}q_{mk}\tau}}\right),$$

$$f_{m3}(\bar{\boldsymbol{q}}) = -\frac{(\ln 2)(D_{m1}+D_{m2})(h_{m1}q_{m1}+h_{m2}q_{m2})}{\beta+(\ln 2)(D_{m1}+D_{m2})\sigma^2 B}, \tag{43}$$

$$\beta = B(h_{m1}q_{m1}+h_{m2}q_{m2})\tau W(\kappa_2), \tag{44}$$

$\kappa_2 = -\frac{(\ln 2)(D_{m1}+D_{m2})\sigma^2}{(h_{m1}q_{m1}+h_{m2}q_{m2})\tau}\mathrm{e}^{-\frac{(\ln 2)(D_{m1}+D_{m2})\sigma^2}{(h_{m1}q_{m1}+h_{m2}q_{m2})\tau}}$, and $W(\cdot)$ is the Lambert-W function.

Based on (41) and (38b), the feasibility problem of (38) reduces to:

$$\text{find} \quad \bar{\boldsymbol{q}}, \tag{45}$$

$$\text{s.t.} \quad \sum_{m=1}^{M}\max\{f_{m1}(\bar{\boldsymbol{q}}), f_{m2}(\bar{\boldsymbol{q}}), f_{m3}(\bar{\boldsymbol{q}})\} \leq 1, \tag{45a}$$

$$0 \leq q_{mj} \leq P_{mj}, \sum_{m=1}^{M}\sum_{j=1}^{2} q_{mj} \leq P_{\max}, \quad \forall m, j. \tag{45b}$$

To ensure that (45) is feasible, we construct the following problem:

$$\min_{\bar{\boldsymbol{q}}} \quad \sum_{m=1}^{M}\sum_{j=1}^{2} q_{mj} \tag{46}$$

$$\text{s.t.} \quad \sum_{m=1}^{M}\max\{f_{m1}(\bar{\boldsymbol{q}}), f_{m2}(\bar{\boldsymbol{q}}), f_{m3}(\bar{\boldsymbol{q}})\} \leq 1, \tag{46a}$$

$$0 \leq q_{mj} \leq P_{mj}, \quad \forall m, j. \tag{46b}$$

Note that (45) is feasible if and only if the optimal objective value of (46) is less than $P_{\max}$. According to property of the inverse function, constraint (46a) is convex and problem (46) is a convex function, which can be effectively solved by using the interior point method. As a result, the algorithm for obtaining the maximum sum-rate of problem (38) is summarized in Algorithm 2, where τ^* is the optimal sum-rate of problem (11).

Algorithm 2. Low-Complexity Sum-Rate Maximization

1: Initialize $\tau_{\min}=0$, $\tau_{\max}=\tau^*$, and the tolerance ϵ.
2: Set $\tau=\frac{\tau_{\min}+\tau_{\max}}{2}$, and calculate f_{m1}, f_{m2} and f_{m3} according to (42) and (43), respectively.
3: If the optimal objective value of (46) is less than $P_{\max}$, problem (38) is feasible, set $\tau_{\min}=\tau$. Otherwise, set $\tau=\tau_{\max}$.
4: If $(\tau_{\max}-\tau_{\min})/\tau_{\max} \leq \epsilon$, terminate. Otherwise, go to step 2.

The complexity of the proposed Algorithm 2 in each step lies in checking the feasibility of problem (38), which involves the complexity of $\mathcal{O}(M^3)$ according to (46). As a result, the total complexity of the proposed Algorithm 2 is $\mathcal{O}(M^3\log_2(1/\epsilon))$, where $\mathcal{O}(\log_2(1/\epsilon))$ is the complexity of the bisection method with accuracy ϵ.

5 Sum-Rate Maximization for Uplink NOMA/FDMA/TDMA

To evaluate the performance gain of the RSMA scheme proposed in Sections 2, 3, and 4, and for comparison purposes, we will solve the sum-rate maximization problems for uplink NOMA, FDMA and TDMA schemes. Note that we provide the problem formulations for uplink NOMA, FDMA and TDMA under a total power constraint, which is an aspect that has not been investigated in the literature.

5.1 NOMA

Without loss of generality, the channel gains are sorted in descending order, i.e., $h_1 \geq h_2 \geq \cdots \geq h_K$. In NOMA, the BS first decodes the messages of users with high channel gains and then decodes the messages of users with low channel gains by subtracting the interference from decoded strong user. The achievable rate of user k with NOMA is calculated as [34]:

$$r_k^{\mathrm{NOMA}} = B\log_2\left(1+\frac{h_k q_k}{\sum_{j=k+1}^{K}h_j q_j+\sigma^2 B}\right), \tag{47}$$

where q_k is the transmit power of user k. The transmission power q_k has a maximum transmit power limit P_k, i.e., we have $q_k \leq P_k, \forall k \in \mathcal{K}$. Since NOMA with time sharing introduces high implementation complexity and synchronization among users, this subsection only considers NOMA without time sharing.

Similar to (8), the sum-rate maximization problem for uplink NOMA can be given by:

$$\max_{\tau, \boldsymbol{q}} \quad \tau, \tag{48}$$

$$\text{s.t.} \quad B\log_2\left(1+\frac{h_k q_k}{\sum_{j=k+1}^{K}h_j q_j+\sigma^2 B}\right) = D_k\tau, \quad \forall k \in \mathcal{K}, \tag{48a}$$

$$0 \le q_k \le P_k, \sum_{k=1}^{K} q_k \le P_{\max}, \quad \forall k \in \mathcal{K}. \tag{48b}$$

To obtain the optimal solution of problem (48), we provide the following theorem.

Theorem 2. *The optimal solution of problem (48) is*

$$\tau^* = \min_{k \in \mathcal{K} \cup \{0\}} \tau_k, \tag{49}$$

and

$$\begin{aligned} q_k^* =& \frac{1}{h_k}\left(2^{\frac{D_k \tau^*}{B}} - 1\right) \sum_{j=k+1}^{K} 2^{\frac{\sum_{l=k+1}^{j-1} D_l \tau^*}{B}} \left(2^{\frac{D_j \tau^*}{B}} - 1\right) \sigma^2 B \\ &+ \frac{1}{h_k}\left(2^{\frac{D_k \tau^*}{B}} - 1\right) \sigma^2 B, \quad \forall k \in \mathcal{K}, \end{aligned} \tag{50}$$

where τ_0 is the solution to

$$\begin{aligned} P_{\max} =& \sum_{k=1}^{K} \left(\frac{1}{h_k}\left(2^{\frac{D_k \tau_0}{B}} - 1\right) \sum_{j=k+1}^{K} 2^{\frac{\sum_{l=k+1}^{j-1} D_l \tau_0}{B}} \right. \\ & \left. \cdot \left(2^{\frac{D_j \tau_0}{B}} - 1\right) \sigma^2 B + \frac{1}{h_k}\left(2^{\frac{D_k \tau_0}{B}} - 1\right) \sigma^2 B \right), \end{aligned} \tag{51}$$

and τ_k is the solution to

$$\begin{aligned} P_k =& \frac{1}{h_k}\left(2^{\frac{D_k \tau_k}{B}} - 1\right) \sum_{j=k+1}^{K} 2^{\frac{\sum_{l=k+1}^{j-1} D_l \tau_k}{B}} \left(2^{\frac{D_j \tau_k}{B}} - 1\right) \sigma^2 B \\ &+ \frac{1}{h_k}\left(2^{\frac{D_k \tau_k}{B}} - 1\right) \sigma^2 B, \quad \forall k \in \mathcal{K}. \end{aligned} \tag{52}$$

Proof. See Appendix E, available in the online supplemental material. □

Since the right hand side of (52) monotonically increases with τ_k, the solution of τ_k to (52) can be effectively obtained by the bisection method.

5.2 FDMA

In FDMA, each user will be allocated a fraction of the BS bandwidth. Let b_k denote the fraction of bandwidth allocated to user k. Then the data rate of user k is:

$$r_k^{\mathrm{FDMA}} = B b_k \log_2\left(1 + \frac{h_k q_k}{\sigma^2 B b_k}\right). \tag{53}$$

Note that user k transmits with maximum power in (53) since there is no inter-user interference and large power leads to high data rate. Due to limited bandwidth, we have $\sum_{k=1}^{K} b_k = 1$.

Similar to (8), the sum-rate maximization problem for uplink FDMA can be given by:

$$\max_{\tau, \boldsymbol{b}, \boldsymbol{q}} \quad \tau, \tag{54}$$

$$\text{s.t.} \quad B b_k \log_2\left(1 + \frac{h_k q_k}{\sigma^2 B b_k}\right) = D_k \tau, \quad \forall k \in \mathcal{K}, \tag{54a}$$

$$\sum_{k=1}^{K} b_k = 1, \tag{54b}$$

$$b_k \ge 0, \quad \forall k \in \mathcal{K}, \tag{54c}$$

$$0 \le q_k \le P_k, \sum_{k=1}^{K} q_k \le P_{\max}, \quad \forall k \in \mathcal{K}, \tag{54d}$$

where $\boldsymbol{b} = [b_1, b_2, \ldots, b_K]^T$. Although problem (54) is nonconvex due to the nonlinear equal constraint (54b), problem (54) is equal to the following convex optimization problem:

$$\max_{\tau, \boldsymbol{b}, \boldsymbol{q}} \quad \tau, \tag{55}$$

$$\text{s.t.} \quad B b_k \log_2\left(1 + \frac{h_k q_k}{\sigma^2 B b_k}\right) \ge D_k \tau, \quad \forall k \in \mathcal{K}, \tag{55a}$$

$$\sum_{k=1}^{K} b_k = 1, \tag{55b}$$

$$b_k \ge 0, \quad \forall k \in \mathcal{K}, \tag{55c}$$

$$0 \le q_k \le P_k, \sum_{k=1}^{K} q_k \le P_{\max}, \quad \forall k \in \mathcal{K}, \tag{55d}$$

where constraint (55a) always holds with equality for the optimal solution as otherwise the objective value can be further improved, which contradicts the fact the solution is optimal. For convex optimization problem (55), the optimal solution can be obtained by using the interior point method.

5.3 TDMA

In TDMA, each user will be assigned a fraction of time to use the whole BS bandwidth. Let a_k be the fraction of time allocated to user k. The data rate of user k is:

$$r_k^{\mathrm{TDMA}} = B a_k \log_2\left(1 + \frac{h_k q_k}{\sigma^2 B}\right), \tag{56}$$

with $\sum_{k=1}^{K} a_k = 1$.

Similar to (8), the sum-rate maximization problem for uplink TDMA can be given by:

$$\max_{\tau, \boldsymbol{a}, \boldsymbol{q}} \quad \tau, \tag{57}$$

$$\text{s.t.} \quad B a_k \log_2\left(1 + \frac{h_k q_k}{\sigma^2 B}\right) \ge D_k \tau, \quad \forall k \in \mathcal{K}, \tag{57a}$$

$$\sum_{k=1}^{K} a_k = 1, \tag{57b}$$

$$a_k \ge 0, \quad \forall k \in \mathcal{K}, \tag{57c}$$

$$0 \le q_k \le P_k, \sum_{k=1}^{K} a_k q_k \le P_{\max}, \quad \forall k \in \mathcal{K}, \tag{57d}$$

where $\boldsymbol{a} = [a_1, a_2, \ldots, a_K]^T$ and constraint (57a) always holds with equality for the optimal solution.

In constraint (57d), $\sum_{k=1}^{K} a_k q_k$ stands for the average transmit power of all users. Due to non-convex constraint (57d), problem (57) is non-convex. To handle the non-convexity of constraint (57 d), we introduce new variables $q_k' = a_k q_k, \ \forall k \in \mathcal{K}$. Since $0 \le q_k \le P_k$, we have $0 \le q_k' \le P_k a_k$. Replacing q_k with q_k', problem (57) is equivalent to:

TABLE 1
System Parameters

Parameter	Value
Bandwidth of the BS B	1 MHz
Noise power spectral density σ^2	-174 dBm/Hz
Path loss model	$128.1+37.6\log_{10}d$ (d is in km)
Standard deviation of shadow fading	8 dB
Maximum transmit power P	1 dBm

$$\max_{\tau,\boldsymbol{a},\boldsymbol{q}'} \quad \tau, \tag{58}$$

$$\text{s.t.} \quad Ba_k \log_2\left(1+\frac{h_k q'_k}{\sigma^2 B a_k}\right) \geq D_k\tau, \quad \forall k\in\mathcal{K}, \tag{58a}$$

$$\sum_{k=1}^{K} a_k = 1, \tag{58b}$$

$$a_k \geq 0, \quad \forall k\in\mathcal{K}, \tag{58c}$$

$$0 \leq q'_k \leq P_k a_k, \sum_{k=1}^{K} q'_k \leq P_{\max}, \quad \forall k\in\mathcal{K}, \tag{58d}$$

where $\boldsymbol{q}' = [q'_1, q'_2, \ldots, q'_K]^T$. In constraint (58a), function $Ba_k \log_2(1+\frac{h_k q'_k}{\sigma^2 Ba_k})$ is concave with respect to (a_k, q'_k) according to the perspective function property [31]. Due to the fact that the objective function and all constraints are convex, problem (58) is convex and the optimal solution can be obtained by using the interior point method.

5.4 Analysis and Discussion

We define the optimal uplink sum-rates for RSMA, NOMA, FDMA and TDMA as τ^{RSMA}, τ^{NOMA}, τ^{FDMA} and τ^{TDMA}, respectively. For the optimal sum-rate with various uplink multiple access schemes, we can state the following lemma.

Lemma 5. $\tau^{\text{RSMA}} \geq \tau^{\text{NOMA}}$ *and* $\tau^{\text{RSMA}} \geq \tau^{\text{FDMA}} \geq \tau^{\text{TDMA}}$.

Lemma 4 can be easily proved by the fact that for any feasible solution to NOMA/FDMA scheme, we can construct a feasible solution to RSMA with the same or better objective value and for any feasible solution to TDMA scheme, we can construct a feasible solution to FDMA with the same or better objective value.

6 Numerical Results

For our simulations, we deploy K users uniformly in a square area of size 500 m $\times$ 500 m with the BS located at its center. The path loss model is $128.1+37.6\log_{10} d$ (d is in km) and the standard deviation of shadow fading is 8 dB. In addition, and the noise power spectral density is $\sigma^2=-174$ dBm/Hz. Unless specified otherwise, we choose an equal maximum transmit power $P_1=\cdots=P_K=P=1$ dBm, maximum transmit power $P_{\max}=KP/2$ dBm. and a bandwidth $B=1$ MHz. The main system parameters are summarized in Table 1. All statistical results are averaged over 10000 independent runs.

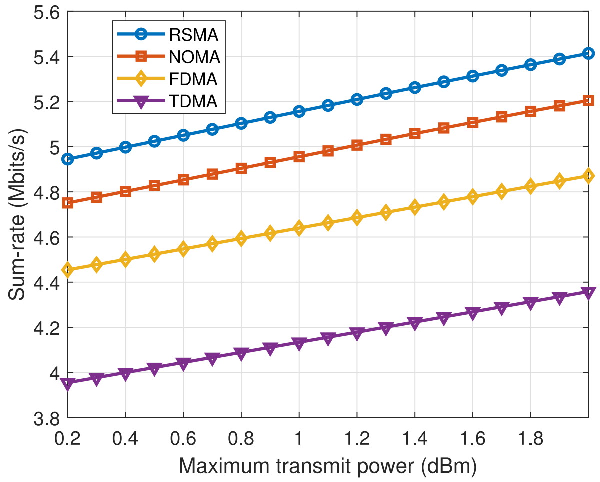

Fig. 4. Sum-rate versus maximum transmit power of each user ($K=2$ users, $D_1=0.5$, and $D_2=0.5$).

We compare the sum-rate performance of RSMA, NOMA, FDMA, and TDMA.[3] Fig. 4 shows how the sum-rate changes as the maximum transmit power of each user varies for a network having two users. We can see that the sum-rate of all multiple access schemes linearly increases with the logarithmic maximum transmission power of each user. This is because the sum-rate is a logarithmic function of the maximum power of the users. It is found that RSMA achieves the best performance among all multiple access schemes. From Fig. 4, RSMA can increase up to 4.1, 10.2 and 26.6 percent sum-rate compared to NOMA, FDMA and TDMA, respectively. This is because that RSMA can achieve the largest rate region and users with RSMA can achieve higher rate than other multiple access schemes. Fig. 4 also shows that TDMA achieves the worst sum-rate performance, which corroborates the theoretical findings in Lemma 5.

Fig. 5 shows the sum-rate versus the bandwidth of the BS. From this figure, we can see that RSMA always achieves a better performance than NOMA, FDMA, and TDMA. Fig. 5 demonstrates that the sum-rate increases rapidly for a small bandwidth, however, this increase becomes slower for a larger bandwidth. This is because a high bandwidth leads to high noise power, which consequently decreases the slope of increase of the sum-rate for all multiple access schemes. Fig. 5 also demonstrates that the sum-rate resulting from RSMA is greater than the one achieved by all other multiple access schemes, particularly when the bandwidth is large.

Fig. 7 shows the sum-rate versus large-scale path loss factor. For all schemes, we find that the sum-rate decreases as the large-scale path loss factor increases. This is due to the fact that, as the large-scale path loss factor increases, the channel gains between the BS and all users become worse.

Fig. 8 shows the sum-rate with different power adjustment errors. In this figure, for scheme "RSMA-ϵ power error

3. For RSMA without user pairing, we run Algorithm 1 under a given decoding order to reduce the complexity. For RSMA with user pairing, the optimal resource allocation is obtained according to Algorithm 2. The power allocation for NOMA, bandwidth allocation for FDMA, and time allocation for TDMA are solved by using the methods of Section 5.

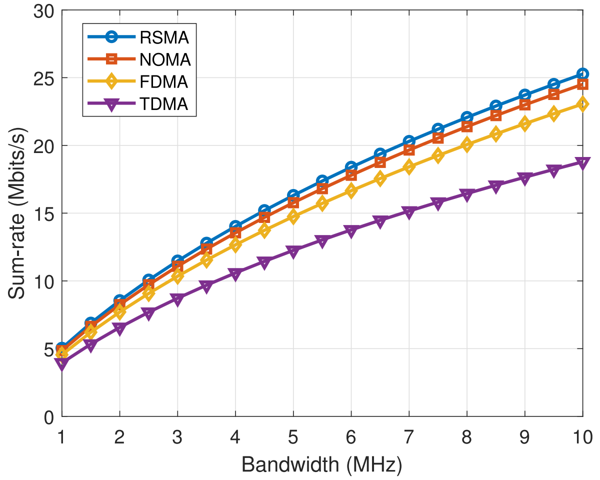

Fig. 5. Sum-rate versus bandwidth of the BS ($K = 2$ users, $D_1 = 0.5$, and $D_2 = 0.5$).

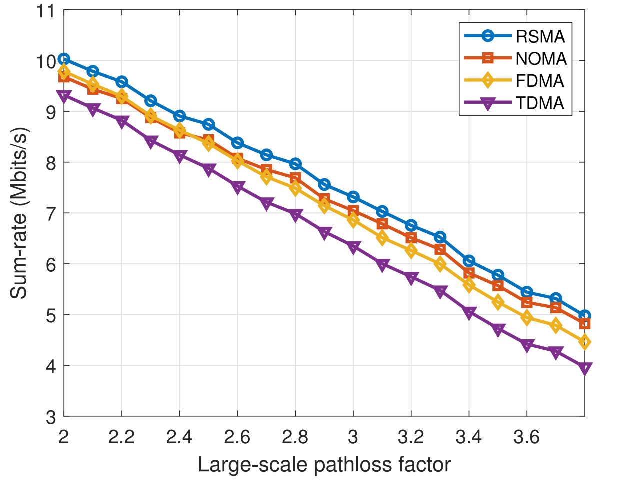

Fig. 7. Sum-rate versus large-scale path loss factor ($K = 2$ users, $D_1 = 0.5$, and $D_2 = 0.5$).

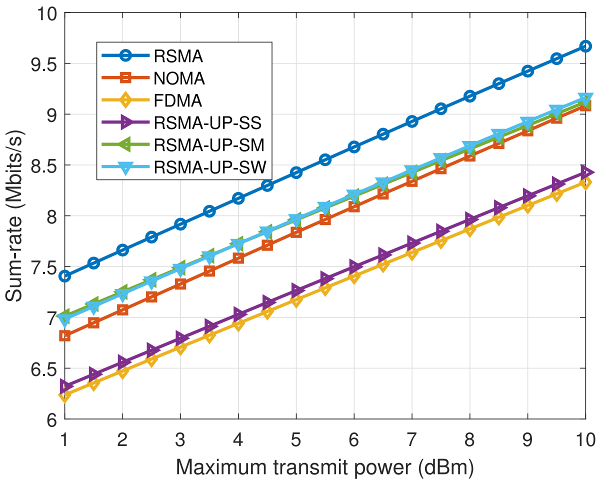

Fig. 6. Sum-rate versus maximum transmit power of each user under different user pairing methods ($K = 10$ users, $D_1 = \cdots = D_{10} = 0.1$).

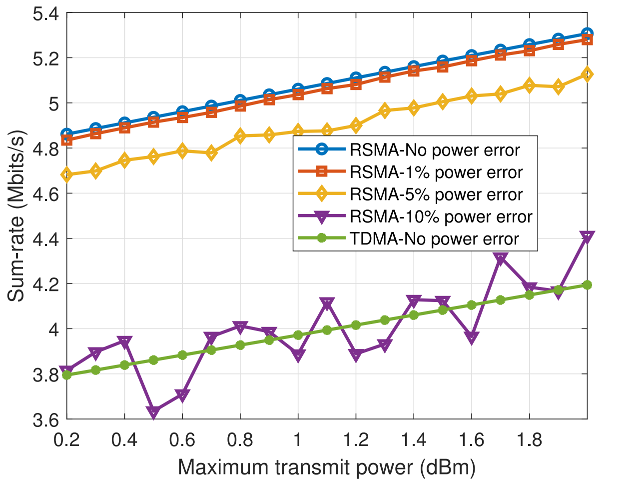

Fig. 8. Sum-rate versus power adjustment error ($K = 2$ users, $D_1 = 0.5$, and $D_2 = 0.5$).

$(\epsilon = 0, 1\%, 5\%, 10\%)$”, we generate the power with error ϵ in RSMA scheme, i.e., we generate power $p_{kj} = p^*_{kj} + \epsilon x p^*_{kj}$, where p^*_{kj} is the optimal transmit power of sub-message s_{kj} from user k, and x is a Gaussian variable with zero mean and unit various. To ensure that the generated power values meet the maximum power constraint, if $\sum_{k=1}^{K}\sum_{j=1}^{2} p_{kj} > P_{\max}$, we set

$$p_{k1} = \frac{p_{k1}}{\sum_{k=1}^{K}\sum_{j=1}^{2} p_{kj}} P_{\max}, p_{k2} = \frac{p_{k2}}{\sum_{k=1}^{K}\sum_{j=1}^{2} p_{kj}} P_{\max}, \tag{59}$$

and if $p_{k1} + p_{k2} > P_k$, we further set

$$p_{k1} = \frac{p_{k1}}{p_{k1+p_{k2}}} P_k, p_{k2} = \frac{p_{k2}}{p_{k1+p_{k2}}} P_k. \tag{60}$$

From Fig. 8, we can see that the rate decreases slightly when the power adjustment error is small (i.e., no more than 1 percent). However, when the power adjustment error is high (i.e., no less than 10 percent), the rate performance of RSMA is even worse than TDMA without power adjustment error.

For low-complexity RSMA with user pairing (labeled as ‘RSMA-UP’), we study the influence of user pairing by considering three different user-pairing methods [33]. For strong-weak (SW) pair selection, the user with the strongest channel condition is paired with the user with the weakest in one pair, and the user with the second strongest is paired with one with the second weakest in one pair, and so on. For strong-middle (SM) pair selection, the user with the strongest channel condition is paired with the user with the middle strongest user in one pair, and so on. For strong-strong (SS) pair selection, the user with the strongest channel condition is paired with the one with the second strongest in one pair, and so on.

In Fig. 6, we show how the sum-rate changes as the maximum transmit power of each user varies for a network having ten users. From this figure, we observe that RSMA always achieves the best performance. For RSMA-UP with different user-pairing methods, SW outperforms the other two methods in terms of sum-rate for RSMA-UP. To maximize the sum-rate, it tends to pair users with distinctive gains for sum-rate maximization. Due to the superiority of SW, we choose SW for pair selection of RSMA-UP in the following simulations.

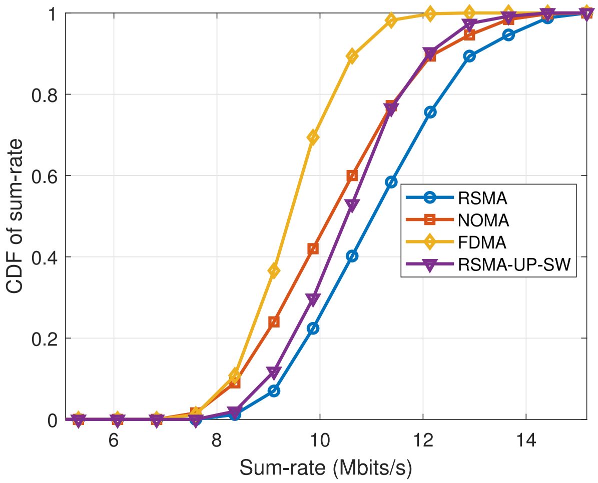

Fig. 9. CDF of sum-rate ($K = 10$ users, $D_1 = \cdots = D_{10} = 0.1$).

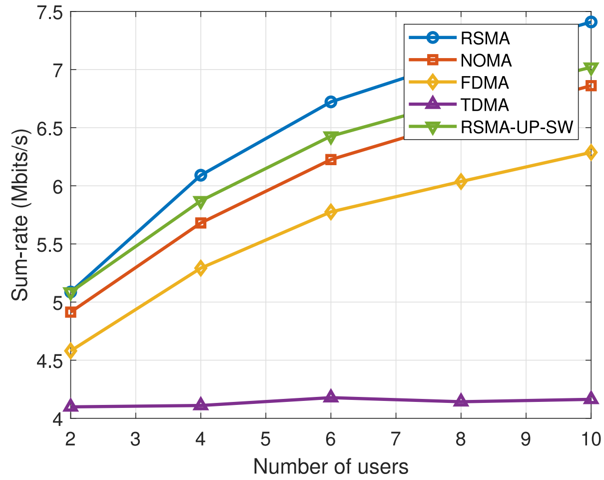

Fig. 10. Sum-rate versus number of users ($D_1 = \cdots = D_K = 1/K$).

Fig. 9 presents the cumulative distribution function (CDF) of sum-rate resulting from RSMA, NOMA, FDMA, and RSMA-UP-SW for a network with $K = 10$ users. From Fig. 9, the CDFs for RSMA, RSMA-UP-SW, and NOMA all improve significantly compared FDMA, particularly when the sum-rate is high, which shows that RSMA, RSMA-UP-SW, and NOMA are suitable for high sum-rate transmission. Moreover, we can observe that RSMA outperforms NOMA. This is because RSMA can adjust the splitting power of two messages for each user so as to control the interference decoding thus optimizing the sum-rate of all users, while there is no power splitting for each user in NOMA. Moreover, RSMA-UP-SW can achieve a similar performance to RSMA. However, the complexity of RSMA-UP-SW is much lower compared to RSMA according to Sections 3.2 and 4, which shows the effectiveness of RSMA-UP-SW.

In Fig. 10, we plot the sum-rate versus the number of users is given. Clearly, the proposed RSMA or RSMA-UP-SW will always achieve a better performance compared to NOMA, FDMA, and TDMA especially when the number of users is large. In particular, RSMA can achieve sum-rate gains of up to 10.0, 22.2, and 81.2 percent compared to NOMA, FDMA, and TDMA, respectively, while RSMA-UP-SW can improve the sum-rate by up to 4.1, 11.6 and 63.5 percent compared to NOMA, FDMA, and TDMA, respectively. When the number of users is large, the multi-user gain is more pronounced for the proposed RSMA compared to conventional NOMA, FDMA, and TDMA. This is due to the fact hat RSMA can effectively determine the power splitting of each user to achieve the theoretically maximal rate region, while there is no power splitting in NOMA and the allocated bandwidth/time of each user is low for FDMA/TDMA when the number of users is large. However, RSMA achieves a better performance compared to NOMA, FDMA, and TDMA at the cost of additional computational complexity according to Section 3.2. Fig. 10 also shows that RSMA-UP-SW achieves a better sum-rate performance compared to NOMA, FDMA, and TDMA but with a lower complexity compared with RSMA without user pairing. Clearly, RSMA-UP-SW is promising solution that strikes a desirable tradeoff between performance gain and computational complexity.

7 Conclusion

In this paper, we have investigated the decoder order and power optimization in an uplink RSMA system. We have formulated the problem as a sum-rate maximization problem. To solve this problem, we have transformed it into an equivalent problem with only rate splitting variables, which has closed-form optimal solution. Given the optimal rate requirement of each user, the optimal transmit power of each user is obtained under given the decoding order and the optimal decoding order is found by an exhaustive search method. To reduce the computational complexity, we have proposed a low-complexity RSMA with user pairing. Simulation results show that RSMA achieves higher sum-rate than NOMA, FDMA, and TDMA.

Acknowledgments

This work was supported in part by the EPSRC through the Scalable Full Duplex Dense Wireless Networks (SENSE) grant EP/P003486/1, and by the U.S. National Science Foundation under Grant CNS-1836802, and by the NSFC under grants 62022026 and 61871109. A preliminary version of this work was accepted by IEEE Globecom 2019 [1].

References

[1] Z. Yang, M. Chen, W. Saad, W. Xu, and M. Shikh-Bahaei, “Sum-rate maximization of uplink rate splitting multiple access (RSMA) communication,” in *Proc. IEEE Global Commun. Conf.*, 2019, pp. 1–6.

[2] W. Saad, M. Bennis, and M. Chen, “A vision of 6G wireless systems: Applications, trends, technologies, and open research problems,” *IEEE Netw.*, vol. 34, no. 3, pp. 134–142, May/Jun. 2019.

[3] Y. Liu, Z. Qin, M. Elkashlan, Z. Ding, A. Nallanathan, and L. Hanzo, “Nonorthogonal multiple access for 5G and beyond,” *Proc. IEEE*, vol. 105, no. 12, pp. 2347–2381, Dec. 2017.

[4] L. Dai, B. Wang, Y. Yuan, S. Han, I. Chih-Lin, and Z. Wang, “Non-orthogonal multiple access for 5G: Solutions, challenges, opportunities, and future research trends,” *IEEE Commun. Mag.*, vol. 53, no. 9, pp. 74–81, Sep. 2015.

[5] Z. Ding, X. Lei, G. K. Karagiannidis, R. Schober, J. Yuan, and V. K. Bhargava, “A survey on non-orthogonal multiple access for 5G networks: Research challenges and future trends,” *IEEE J. Sel. Areas Commun.*, vol. 35, no. 10, pp. 2181–2195, Oct. 2017.

[6] Z. Yang, C. Pan, W. Xu, Y. Pan, M. Chen, and M. Elkashlan, “Power control for multi-cell networks with non-orthogonal multiple access,” *IEEE Trans. Wireless Commun.*, vol. 17, no. 2, pp. 927–942, Feb. 2018.

[7] L. Yang *et al.*, "Cooperative non-orthogonal layered multicast multiple access for heterogeneous networks," *IEEE Trans. Commun.*, vol. 67, no. 2, pp. 1148–1165, Feb. 2019.

[8] B. Clerckx, H. Joudeh, C. Hao, M. Dai, and B. Rassouli, "Rate splitting for MIMO wireless networks: A promising PHY-layer strategy for LTE evolution," *IEEE Commun. Mag.*, vol. 54, no. 5, pp. 98–105, May 2016.

[9] B. Clerckx, Y. Mao, R. Schober, and H. V. Poor, "Rate-splitting unifying SDMA, OMA, NOMA, and multicasting in MISO broadcast channel: A simple two-user rate analysis," *IEEE Wireless Commun. Lett.*, vol. 9, no. 3, pp. 349–353, Nov. 2020.

[10] J. Cao and E. M. Yeh, "Asymptotically optimal multiple-access communication via distributed rate splitting," *IEEE Trans. Inf. Theory*, vol. 53, no. 1, pp. 304–319, Jan 2007.

[11] M. Dai, B. Clerckx, D. Gesbert, and G. Caire, "A rate splitting strategy for massive MIMO with imperfect CSIT," *IEEE Trans. Wireless Commun.*, vol. 15, no. 7, pp. 4611–4624, Jul. 2016.

[12] Y. Mao, B. Clerckx, and V. O. K. Li, "Rate-splitting multiple access for downlink communication systems: Bridging, generalizing, and outperforming SDMA and NOMA," *EURASIP J. Wireless Commun. Netw.*, vol. 2018, no. 1, May 2018, Art. no. 133.

[13] Y. Mao, B. Clerckx, and V. O. Li, "Rate-splitting for multi-user multi-antenna wireless information and power transfer," in *Proc. IEEE Int. Workshop Signal Process. Advances Wireless Commun.*, 2019, pp. 1–5.

[14] A. A. Ahmad, H. Dahrouj, A. Chaaban, A. Sezgin, and M. Alouini, "Interference mitigation via rate-splitting and common message decoding in cloud radio access networks," *IEEE Access*, vol. 7, pp. 80350–80365, 2019.

[15] Y. Mao, B. Clerckx, and V. O. K. Li, "Energy efficiency of rate-splitting multiple access, and performance benefits over SDMA and NOMA," in *Proc. IEEE 15th Int. Symp. Wireless Commun. Syst.*, 2018, pp. 1–5.

[16] A. Rahmati, Y. Yapıcı, N. Rupasinghe, I. Guvenc, H. Dai, and A. Bhuyany, "Energy efficiency of RSMA and NOMA in cellular-connected mmwave UAV networks," in *Proc. IEEE Int. Conf. Commun. Workshops*, 2019, pp. 1–6.

[17] C. Hao, Y. Wu, and B. Clerckx, "Rate analysis of two-receiver MISO broadcast channel with finite rate feedback: A rate-splitting approach," *IEEE Trans. Commun.*, vol. 63, no. 9, pp. 3232–3246, Sep. 2015.

[18] Z. Yang, M. Chen, W. Saad, and M. Shikh-Bahaei, "Optimization of rate allocation and power control for rate splitting multiple access (RSMA)," 2019, *arXiv: 1903.08068*.

[19] H. Joudeh and B. Clerckx, "Sum-rate maximization for linearly precoded downlink multiuser MISO systems with partial CSIT: A rate-splitting approach," *IEEE Trans. Commun.*, vol. 64, no. 11, pp. 4847–4861, Nov. 2016.

[20] H. Joudeh and B. Clerckx, "Robust transmission in downlink multiuser MISO systems: A rate-splitting approach," *IEEE Trans. Signal Process.*, vol. 64, no. 23, pp. 6227–6242, Dec. 2016.

[21] X. Su, L. Li, H. Yin, and P. Zhang, "Robust power- and rate-splitting-based transceiver design in k -user MISO SWIPT interference channel under imperfect CSIT," *IEEE Communi. Lett.*, vol. 23, no. 3, pp. 514–517, Mar. 2019.

[22] Y. Mao, B. Clerckx, and V. O. K. Li, "Rate-splitting for multi-antenna non-orthogonal unicast and multicast transmission: Spectral and energy efficiency analysis," *IEEE Trans. Commun.*, vol. 67, no. 12, pp. 8754–8770, Sep. 2019.

[23] B. Rimoldi and R. Urbanke, "A rate-splitting approach to the Gaussian multiple-access channel," *IEEE Trans. Inf. Theory*, vol. 42, no. 2, pp. 364–375, Mar. 1996.

[24] Y. Zhu, X. Wang, Z. Zhang, X. Chen, and Y. Chen, "A rate-splitting non-orthogonal multiple access scheme for uplink transmission," in *Proc. Int. Conf. Wireless Commun. Signal Process.*, 2017, pp. 1–6.

[25] J. Zeng, T. Lv, W. Ni, R. P. Liu, N. C. Beaulieu, and Y. J. Guo, "Ensuring maxcmin fairness of UL SIMO-NOMA: A rate splitting approach," *IEEE Trans. Vehicular Technol.*, vol. 68, no. 11, pp. 11 080–11 093, Nov. 2019.

[26] H. Liu, T. A. Tsiftsis, K. J. Kim, K. S. Kwak, and H. V. Poor, "Rate splitting for uplink NOMA with enhanced fairness and outage performance," *IEEE Transa. Wireless Commun.*, vol. 19, no. 7, pp. 4657–4670, Jul. 2020.

[27] X. Mao, H. Chen, and P. Qiu, "An algorithm to realize rate-splitting in gaussian multi-access channel," 2016, *arXiv:1608.03663*.

[28] Y. Dong, M. J. Hossaini, J. Cheng, and V. C. Leung, "Robust energy efficient beamforming in MISOME-SWIPT systems with proportional secrecy rate," *IEEE J. Sel. Areas Commun.*, vol. 37, no. 1, pp. 202–215, Jan. 2019.

[29] R. K. Jain, D. M. W. Chiu, and W. R. Hawe, "A quantitative measure of fairness and discrimination," Eastern Research Laboratory, Digital Equipment Corporation, Hudson, MA, 1984.

[30] S. Adireddy, L. Tong, and H. Viswanathan, "Optimal placement of training for frequency-selective block-fading channels," *IEEE Trans. Inf. Theory*, vol. 48, no. 8, pp. 2338–2353, Aug. 2002.

[31] S. Boyd and L. Vandenberghe, *Convex Optimization*. Cambridge, U.K.: Cambridge Univ. Press, 2004.

[32] F. Fang, H. Zhang, J. Cheng, and V. C. M. Leung, "Energy-efficient resource allocation for downlink non-orthogonal multiple access network," *IEEE Trans. Commun.*, vol. 64, no. 9, pp. 3722–3732, Sep. 2016.

[33] Z. Ding, P. Fan, and H. V. Poor, "Impact of user pairing on 5G nonorthogonal multiple-access downlink transmissions," *IEEE Trans. Veh. Technol.*, vol. 65, no. 8, pp. 6010–6023, Aug. 2016.

[34] Y. Saito, Y. Kishiyama, A. Benjebbour, T. Nakamura, A. Li, and K. Higuchi, "Non-orthogonal multiple access (NOMA) for cellular future radio access," in *Proc. IEEE Veh. Technol. Conf.*, 2013, pp. 1–5.

Zhaohui Yang (Member, IEEE) received the BS degree in information science and engineering from Chien-Shiung Wu Honors College, Southeast University, Nanjing, China, in Jun. 2014, and the PhD degree in communication and information system from the National Mobile Communications Research Laboratory, Southeast University, Nanjing, China, in May 2018. He is currently a postdoctoral research associate at the Center for Telecommunications Research, Department of Informatics, King's College London, U.K., where he has been involved in the EPSRC SENSE Project. He has guest edited a 2020 IEEE Feature topic of the *IEEE Communications Magazine on Communication Technologies for Efficient Edge Learning*. He serves as the co-chair for IEEE International Conference on Communications (ICC), 1st Workshop on Edge Machine Learning for 5G Mobile Networks and Beyond, June 2020, IEEE International Symposium on Personal, Indoor and Mobile Radio Communication (PIMRC) Workshop on Rate-Splitting and Robust Interference Management for Beyond 5G, August 2020. His research interests include federated learning, reconfigurable intelligent surface, UAV, MEC, energy harvesting, and NOMA. He was a TPC member of IEEE ICC during 2015-2020 and Globecom during 2017-2020. He was an exemplary reviewer for the *IEEE Transactions on Communications*, in 2019.

Mingzhe Chen (Member, IEEE) received the PhD degree from the Beijing University of Posts and Telecommunications, Beijing, China, in 2019. From 2016 to 2019, he was a visiting researcher with the Department of Electrical and Computer Engineering, Virginia Tech. He is currently a postdoctoral researcher at the Electrical Engineering Department, Princeton University and at The Chinese University of Hong Kong, Shenzhen, China. His research interests include federated learning, reinforcement learning, virtual reality, unmanned aerial vehicles, and wireless networks. He was a recipient of the IEEE International Conference on Communications (ICC) 2020 Best Paper Award and an exemplary reviewer for the *IEEE Transactions on Wireless Communications* in 2018 and the *IEEE Transactions on Communications* in 2018 and 2019. He has served as a co-chair for workshops on edge learning and wireless communications in several conferences including IEEE ICC, IEEE Global Communications Conference, and IEEE Wireless Communications and Networking Conference. He currently serves as an associate editor for Frontiers in Communications and Networks, Specialty Section on Data Science for Communications and a guest editor for *IEEE Journal on Selected Areas in Communications* (JSAC) Special Issue on Distributed Learning over Wireless Edge Networks.

Walid Saad (Fellow, IEEE) received the PhD degree from the University of Oslo, in 2010. He is currently a professor at the Department of Electrical and Computer Engineering at Virginia Tech, where he leads the Network Science, Wireless, and Security (NEWS) laboratory. His research interests include wireless networks, machine learning, game theory, security, unmanned aerial vehicles, cyber-physical systems, and network science. He is an IEEE Distinguished Lecturer. He is also the recipient of the NSF CAREER award in 2013, the AFOSR summer faculty fellowship in 2014, and the Young Investigator Award from the Office of Naval Research (ONR) in 2015. He was the author/co-author of nine conference best paper awards at WiOpt in 2009, ICIMP in 2010, IEEE WCNC in 2012, IEEE PIMRC in 2015, IEEE SmartGridComm in 2015, EuCNC in 2017, IEEE GLOBECOM in 2018, IFIP NTMS in 2019, and IEEE ICC in 2020. He is the recipient of the 2015 Fred W. Ellersick Prize from the IEEE Communications Society, of the 2017 IEEE ComSoc Best Young Professional in Academia award, of the 2018 IEEE ComSoc Radio Communications Committee Early Achievement Award, and of the 2019 IEEE ComSoc Communication Theory Technical Committee. He was also a co-author of the 2019 IEEE Communications Society Young Author Best Paper. From 2015-2017, he was named the Stephen O. Lane Junior Faculty Fellow at Virginia Tech and, in 2017, he was named College of Engineering Faculty Fellow. He received the Dean's award for Research Excellence from Virginia Tech in 2019. He currently serves as an editor for the *IEEE Transactions on Wireless Communications*, the *IEEE Transactions on Mobile Computing*, and the *IEEE Transactions on Cognitive Communications and Networking*. He is also an editor-at-large for the *IEEE Transactions on Communications*.

Wei Xu (Senior Member, IEEE) received the BSc degree in electrical engineering and the MS and PhD degrees in communication and information engineering from Southeast University, Nanjing, China, in 2003, 2006, and 2009, respectively. Between 2009 and 2010, he was a postdoctoral research fellow with the Department of Electrical and Computer Engineering, University of Victoria, Canada. He is currently a professor at the National Mobile Communications Research Laboratory, Southeast University. He is also an adjunct professor with the University of Victoria in Canada, and a distinguished visiting fellow with the Royal Academy of Engineering, United Kingdom. He has co-authored more than 100 refereed journal papers in addition to 36 domestic patents and four US patents granted. His research interests include cooperative communications, information theory, signal processing and machine learning for wireless communications. He was an editor of the *IEEE Communications Letters* from 2012 to 2017. He is currently an editor of the *IEEE Transactions on Communications* and the *IEEE Access*. He received the Best Paper Awards from IEEE MAPE 2013, IEEE/CIC ICCC 2014, IEEE Globecom 2014, IEEE ICUWB 2016, WCSP 2017, and ISWCS 2018. He was the co-recipient of the First Prize of the Science and Technology Award in Jiangsu Province, China, in 2014. He received the Youth Science and Technology Award of China Institute of Communications in 2018.

Mohammad Shikh-Bahaei (Senior Member, IEEE) received the BSc degree from the University of Tehran, Tehran, Iran, in 1992, the MSc degree from the Sharif University of Technology, Tehran, Iran, in 1994, and the PhD degree from King's College London, U.K., in 2000. He has worked for two start-up companies, and for National Semiconductor Corp., Santa Clara, CA, (now part of Texas Instruments Incorporated), on the design of third-generation (3G) mobile handsets, for which he has been awarded three U.S. patents as inventor and co-inventor, respectively. In 2002, he joined King's College London as lecturer, and is now a full professor with Telecommunications at the Center for Telecommunications Research, Department of Engineering, King's College London. He has since authored or co-authored numerous journal and conference articles. He has been engaged in research in the area of wireless communications and signal processing for 25 years both in academic and industrial organizations. His research interests include the fields of Learning based resource allocation for multimedia applications over heterogeneous communication networks, Full Duplex and UAV communications, and Secure communication over wireless networks. Prof. Shikh-Bahaei was the Founder and Chair of the Wireless Advanced (formerly SPWC) Annual International Conference from 2003 to 2012. He was the recipient of the overall King's College London Excellence in Supervisory Award, in 2014.